DOI: 10.1002/((adma.201606806))
Article type: Communication

Isomer-pure bis-PCBM assisted crystal engineering of perovskite solar cells showing excellent efficiency and stability

Fei Zhang, Wenda Shi, Jingshan Luo, Norman Pellet , Chenyi Yi, Xiong Li, Xiaoming Zhao, T. John S. Dennis, Xianggao Li, Shirong Wang*, Yin Xiao, Shaik Mohammed Zakeeruddin, Dongqin Bi*, Michael Grätzel**

F. Zhang, X. Zhao, Prof. X. Li, Prof. S. Wang*, Dr.Y.Xiao,
School of Chemical Engineering and Technology, Tianjin University
300072 Tianjin, China
Email: wangshirong@tju.edu.cn

F. Zhang, Dr. J. Luo, N.Pellet, Dr. C. Yi,Dr. X. Li, Dr. S. M. Zakeeruddin, Dr. D. Bi *, Prof. M. Grätzel*
Laboratory of Photonics and Interfaces, Institute of Chemical Sciences and Engineering,
École Polytechnique Fédérale de Lausanne (EPFL)
Station 6 CH-1015, Lausanne, Switzerland
Email: dongqin.bi@epfl.ch ; michael.graetzel@epfl.ch

F. Zhang, X. Zhao, Prof. X. G. Li, Prof. S. Wang*, Dr.Y.Xiao,
Collaborative Innovation Center of Chemical Science and Engineering(Tianjin)
300072 Tianjin, China

Dr.W. Shi, X. Zhao, Dr. T. J. S. Dennis*
School of Physics and Astronomy, Queen Mary University of London,
327 Mile End RoadLondon, E1 4NS, UK
Email: j.dennis@qmul.ac.uk

Keywords: stability; bis-PCBM; perovskite; solar cell

Abstract: The fullerene derivative (α-bis-PCBM) was purified from an as-produced bis-phenyl-C_{61}-butyric acid methyl ester (bis-[60]PCBM) isomer mixture by preparative peak-recycling high performance liquid chromatography (HPLC) and employed as a templating agent for solution processing of metal halide perovskite films *via* an antisolvent method. The resulting α-bis-PCBM-containing perovskite solar cells (PSCs) achieve better stability, efficiency, and reproducibility when compared with analogous cells containing PCBM. α-bis-PCBM fills the vacancies and grain boundaries of the perovskite film, enhancing the crystallization of perovskites and addressing the issue of slow electron extraction. In addition,

α-bis-PCBM resists the ingression of moisture and passivates voids or pinholes generated in the hole-transporting layer. As a result, we obtain a power conversion efficiency (PCE) of 20.8 % compared with 19.9 % by PCBM, accompanied by excellent stability under heat and simulated sunlight. The PCE of unsealed devcies dropped by less than 10% in ambient air (40% RH) after 44 days at 65℃ and by 4% after 600 h under continuous full sun illuminationand maximum power point tracking respectively.

Hybrid organic-inorganic lead halide perovskite solar cells (PSCs) have emerged as a promising candidate for the next generation photovoltaic technology. This is primarily due to their low manufacturing cost and high performance.[1–6] Through judicious manipulation of perovskite morphology and improvement of interfacial properties,[2–6] PSCs have reached a certified power conversion efficiency (PCE) up to 22.1%.[7] Generally, the PSCs with the best performance employ a sandwich-type configuration, composed of a layer of TiO_2 electron selective contact that is infiltrated by an intrinsic perovskite light harvester, followed by a layer of hole transport material (HTM) as a p-type contact, and a metal back contact.[8]

Despite of these stunning advances, several challenges still remain before PSCs become a competitive commercial technology, one crucial issue being device stability.[9–11] Uncontrolled film morphology associated with poor crystallity of perovskites results in low efficiency and poor device performance reproducibility.[12] Previous studies indicate that the degradation of PSCs is primarily governed by ingress of atmospheric oxygen and water vapor into the film upon exposure to air, which in turn causes undesired reactions with the active materials.[13,14] Various methods have been tried to modify the morphology of perovskite films aiming at improving stability. For example, poly(methyl methacrylate) (PMMA) was used as a template to control nucleation and crystal growth, resulting in considerable increase in both the device efficiency and stability when kept under dry condition in the dark. [15] Other studies use additives like 1-methyl-3-(1H,1H,2H,2H-nonafluorohexyl)-imidazolium iodide,[16] or

phenyl-C_{61}-butyric acid methyl ester (PCBM)[17-19] or alkali metal ions[20] in the pervokite precursor solution to improve film formation and increase environmental stability. However, very few investigations achieve stability under both prolonged heat and light soaking stress where the resulting PSCs exhibiting a high PCE and good moisture resistance.[21]

A bis-analogue of PCBM, bis-PCBM, was successfully utilized in polymer solar cells to improve the open-circuit voltage (V_{oc}) over simple PCBM.[22,23] However, the increase in PCE is not as high as expected from the increase in $V_{oc,}$ which is because that bis-PCBM may exists as a mixture of up to 21 dicyclopropafullerene-type isomers, which leads to morphological and energetic disorder in the active layer of photovoltaic devices with a resulting degrading effect on the short circuit current density (J_{sc}).[24] The disorders induced by the isomer mixture may be removed through fabricating devices from isomer-pure samples. Hence, using isomer-pure samples may potentially lead to both higher voltage and higher current in the polymer solar cells, compared to the isomer mixture.[25]

Some of us have recently purified 18 isomers from the mixture by preparative peak-recycling HPLC,[26] and herein, we have employed the most abundant of those isomers, α-bis-PCBM, as a templating agent in the chlorobenzene antisolvent to enhance the electronic quality and PV performance of solution processed perovskite films. Our results show that the α-bis-PCBM leads to (i) enlargement of the perovskite grain size, (ii) passivation of the interface trap states at the grain boundaries, and (iii) improvement of the charge carrier separation and transportation within the perovskite film.[27-29] Thus, PSCs using α–bis-PCBM as an additive in the antisolvent to template the nucleation and growth of the PSC attained a PCE of 20.8 %, compared with 18.8 % for the PCBM-free reference and 19.9 % for PCBM itself. Importantly, this PCE increase is accompanied by enhanced stability under heat and illumination.

Figure 1 shows a schematic illustration of the α–bis-PCBM-assisted (or PCBM-assisted) growth process for the perovskite-α–bis-PCBM (or PCBM) layer. The mixed cation perovskite [$(FAI)_{0.81}(PbI_2)_{0.85}(MABr)_{0.15}(PbBr_2)_{0.15}$] films are produced in a single step from a solution of formamidinium iodide (FAI), PbI_2, methylammonium bromide (MABr) and $PbBr_2$ in a mixed solvent of dimethyl formamide (DMF) and dimethyl sulfoxide (DMSO). The perovskite spin-coating procedure employed 2000 rpm for 10 s followed by 6000 rpm for 30 s. During the last 15 s of second spin coating step 100 ml of α–bis-PCBM containing chlorobenzene (CB) was dropped onto the above film to template the nucleation and growth of the perovskite crystals.

Figure S2 shows scanning electron microscopy (SEM) images of the corresponding perovskite films deposited on m-TiO_2/c-TiO_2/FTO substrate. As illustrated from the top-view SEM, the grain size of the perovskite film increases with the use of either PCBM or α–bis-PCBM and directs most of the grain boundaries to assume a perpendicular orientation to the substrate. Hence, PCBM or α–bis-PCBM is expected to uniformly trigger heterogeneous nucleation over the perovskite precursor film – improving the grain size and facilitating the perovskite to grow in preferred direction. The XRD pattern (**Figure 2a**) indicates that reflections of facets with (111) indices become dominant because of the low symmetry of the trigonal perovskite (p3m1) phase;[15] whereas, the cross-sectional SEM of the reference film reveals numerous grain boundaries, very few appear in the PCBM or α–bis-PCBM-containing film. High-angle annular dark-field scanning transmission electron microscopy (HAADF-STEM), shown in **Figure S3**, indicates that the α–bis-PCBM can fill in the vacancies and grain boundaries of the perovskite film. **Figure S4** shows the results of our measured the contact angle between the corresponding films and CB. The angle of the CB droplet on the α-bis-PCBM containing film was 61.70°. This can be compared with 69.40° for PCBM and

73.46° for the control – indicating better wetting of the α–bis-PCBM containing perovskite by the CB when compared with the other two samples.[11]

The crystal structure of the perovskite films characterized by thin film X-ray diffraction (XRD) measurements on m-TiO_2/c-TiO_2/FTO substrates (**Figure 2a**). All the samples show the same trigonal perovskite phase with the dominant (111) lattice reflection. The peak at 12.5° arises from the (001) lattice planes of PbI_2. The excess PbI_2 is believed to passivate surface defects, increasing the solar cell performance.[30,31] By taking the full width at half maximum (FWHM) of the (111) reflection we calculated the crystallite size using Scherrer's equation. Their size increases from 38 nm to 49 nm and 67 nm for the control, PCBM and α-bis-PCBM respectively. We attribute the larger crystal sizes to the templating effect of PCBM or α-bis-PCBM on the crystal growth. These observations indicate that α-bis-PCBM-containing perovskite film has a higher crystal quality. We ascribe the high-quality crystallization as one of the main factors for improved device performance.[32-34]

We exposed unsealed films of pristine, PCBM and α-bis-PCBM-containing perovskite to ambient environments, and periodically recorded their thin film X-ray diffraction patterns. The decomposition of perovskite in moist air is known to lead to the formation of a PbI_2 phase.[35] XRD patterns (**Figure 2a**) the ratio of PbI_2 ($2\theta = 12.5°$) to perovskite ($2\theta = 13.8°$) of pristine control perovskite increases faster than that of PCBM-containing and α-bis-PCBM-containing perovskite film after 40 days. The α-bis-PCBM-containing perovskite film turned out to be the most stable one in this test environment. The enhanced stability of the α-bis-PCBM-containing perovskite film can also be seen from the **Figure 2b**, which shows that the color of the α-bis-PCBM-containing perovskite films remain persistent; whereas, those of the PCBM-containing and pristine control perovskite film fade from black to yellow. **Figure 2c** shows contact-angle measurements of a deionized water droplet with the pristine control, PCBM and α-bis-PCBM-containing perovskite film. The derived contact angles are 71.56°,

63.30° and 47.10° for the α-bis-PCBM, PCBM-containing film and the pristine control respectively. This trend reflects a strong increase in hydrophobicity of the perovskite upon incorporation of the α–bis-PCBM providing a rational for its greatly enhanced stability against degradation in humid air.

To understand the large enhancement of PCE in the mixed perovskite solar cells, we performed photoluminescence (PL) characterizations for the corresponding samples on a glass substrate. The introduction of an electron-accepting fullerene into the perovskite layer should largely quench the PL for ensuring fast electron-collection efficiency in complete devices.[18,36] As is shown in **Figure 3a**, the sample with a PCBM-containing perovskite layer quenches the PL by 54%, while that with the α-bis-PCBM-containing sample quenches the PL by 79%, which is a very substantial increase. When compared with the pristine perovskite film, the normalized the steady-state PL spectra, shown in **Figure S5a**, indicates blue shifting of 1 nm and 4 nm for PCBM-containing and α-bis-PCBM–containing perovskite layers, respectively. This is probably the origin of enhanced V_{oc} – because such blue shifting and line narrowing is attributed to decrease of spontaneous radiative recombination between trap states.[37]

Figure 3b shows time-resolved PL decay measurements and the stretched exponential decay lifetimes were obtained by fitting the data with an biexponential decay function.[37] The α-bis-PCBM-containing and PCBM-containing perovskite film respectively show fast and slow phase lifetimes of (τ_1 = 15.4 ns , τ_2 = 726.2 ns) and (τ_1 = 7.3 ns , τ_2 = 621.9 ns). By contrast, the pristine perovskite film gave τ_1 = 4.6 ns and τ_2 = 303.1 ns for these lifetimes. This indicates a lower defect concentration, and hence superior electronic quality, for the α-bis-PCBM-containing perovskite film, which again is consistent with the higher V_{oc} of the corresponding PSC.[36]

Perovskite solar cells with the structure of Au/SpiroOMeTAD/ perovskite /mesoporous TiO_2/compact TiO_2/FTO were fabricated. A cross sectional scanning electron microscopy

(SEM) image of which is shown in **Figure 4a**. **Figure 4b** shows the *J–V* characteristics of pristine perovskite, PCBM-containing and α-bis-PCBM-containing perovskite layer-based PSCs under AM 1.5 G illumination with the light intensity of 100 mW cm^{-2}. The key cell parameters are summarized in **Table S1**. A control device based on pristine perovskite gave a J_{sc} of 23.32 mA cm^{-2}, a V_{oc} of 1.09 V, a fill factor (*FF*) of 0.71, and a PCE of 18.8 %. These values are comparable with a previous report.[5] In contrast, PCBM-containing and α–bis-PCBM-containing perovskite-based devices exhibit significant improvements in both J_{sc} ,*Voc* and *FF*. The PCBM-containing perovskite-based solar cells presented better performance with PCE of 19.9 %, J_{sc} of 23.73 mA cm^{-2}, V_{oc} of 1.11 V, and *FF* of 0.73, while the α–bis-PCBM-containing perovskite-based solar cells present the best performance with a PCE of 20.8 %, J_{sc} of 23.95 mA cm^{-2}, V_{oc} of 1.13 V, and *FF* of 0.74. As previously reported,[38,39] PCBM plays a critical role in improving the quality of the active layer with large grains and fewer grain boundaries, which result in obviously enhanced J_{sc} and *FF*. This study shows that α-bis-PCBM gives a substantially greater enhancement. We ascribed the improvement in J_{sc} with α-bis-PCBM to be mainly due to improved photoelectron transport speed [**Figure S5b**], higher conductivity, higher mobility [**Table S2**] and no obvious boundaries. *J-V* curves, shown in **Figure 4b**, indicate that commonly observed hysteresis[40] is virtually negligible in our devices. The stabilized power outputs from devices based on pristine perovskite, PCBM-containing and α-bis-PCBM-containing perovskite layer are 18.6 %, 19.7 % and 20.7 % respectively (**Figure 4d**), which is consistent with the obtained PCEs.

The incident photon-to-electron conversion efficiency (IPCE) spectra of the cells based on the corrosponding perovskite layers are presented in **Figure 4c**. The integrated current densities estimated from the IPCE spectra are: 21.7 mA cm^{-2}, 22.3 mA cm^{-2} and 22.8 mA cm^{-2} for pristine control, PCBM-containing and α-bis-PCBM-containing perovskite layer-based solar cells, respectively. These are in good agreement with the J_{sc} values obtained from the *J-*

V curves. The reproducibility of the device performance was evaluated by characterizing about 20 cells. Histograms of the PCE parameters of these devices (**Figures 3c**, **d**, **e**, **f**) indicate excellent reproducibility.

Degradation of perovskite solar cells is mainly associated with two processes. The first is decomposition of the active layer *via* corrosion by moisture that intrudes into the active layer through the degraded top electrode;[41,42] and the second is current leakage caused by the formation of hot spots in the bulk or at the interface.[43] **Figure 5** and **S6,** and **S7** shows the results of stability tests of the corresponding perovskite solar cells under an ambient environment of 40% relatively humidity without encapsulation, an ambient environment of 40% relative humidity at 65℃ with encapsulation and under continuous full sun illumination, and at the maximum power point tracking under a nitrogen atmosphere at room temperature without encapsulation, respectively. It is clear from these tests that, although the PCBM-containing perovskite based device give better stability than that of the pristine control perovskite device, the α-bis-PCBM-containing perovskite based device presents a further and very substantial increase in stability. For example, **Figure 5a** shows the α-bis-PCBM-containing perovskite-based device maintained 90.1% of its initial PCE after 44 days without encapsulation days; whereas under the same conditions the measured PCEs decreased to 45.4% and 72.6% of their initial values in the pristine control perovskite and PCBM-containing perovskite based solar cells, respectively. The devices with an α-bis-PCBM-containing perovskite layer exhibited negligible degradation (less than 10%) upon exposure to air for 44 days at 65℃ shown in **Figure 5b**. Moreover, preliminary tests in **Figure S7** shows that the α-bis-PCBM-containing perovskite-based device is more resistant to heat stress than the device based on PCBM-containing and pristine control perovskite at 85℃. **Figure 5c** indicates that there is only a 4% efficiency drop after 600 h continuous full sun illumination at maximum power point tracking for α-bis-PCBM-containing perovskite solar cell. We ascribe

the improved stability from α-bis-PCBM-containing perovskite as being mainly due to the presence of less pinholes in the spiro-OMeTAD layer (**Figure S9**), layer grain size and no obvious boundaries.[8,9,44,45] As a result, the α-bis-PCBM-containing perovskite device showed a much stronger resistance to degradation over a much longer time periods than the other two corresponding devices (as indicated in **Figure 5** and **S6-S8**).

In conclusion, We have demonstrated PSCs with simultaneously improved device performance and stability based on a one-step solution-processable strategy by a facile α-bis-PCBM-containing perovskite growth method during the device fabrication. The α-bis-PCBM network resists moisture incursion, thus preventing erosion of the interfaces and passivating the voids or pinholes generated in the bulk active layer. The introduction of α-bis-PCBM also positively addresses the issues of low electron extraction efficiency, enhance the crystallization of perovskites, and improve the stability of the PSCs. This promising approach provides a simple route for the fabrication of highly efficient and stable bulk heterojunction perovskite solar cells.

Supporting Information

Supporting Information is available from the Wiley Online Library or from the author.

Author contributions

F.Z. and D.Q.B designed the experiment. F.Z carried out the experimental study on device fabrication and performed basic characterization. W.S., X.Z. and T.J.S.D. synthesized and purified the the bis-PCBM. F.Z. performed the PL and contact angle test. N.M and F.Z performed the stability test. C.Y.Y and X. L performed the IPCE test. J.S.L. performed SEM and XRD measurements. Z.F wrote the first draft of the paper. All the

authors contributed to the discussion and the writing of the paper, and approved. S.M.Z. and X.G.L coordinated the research, whereas S.R.W. and M.G. supervised the project.

Acknowledgements:

We thank Dr. Giordano Fabrizio (LPI) in help with the IMPS test and Mr.Linfeng Pan(LSPM) for hall effect test. FZ, WS and XZ thank the China Scholarship Council for funding. TJSD thanks the EPSRC for a Joint QMUL/Warwick Award for Collaborative Research Projects. SRW and XGL thank the National Natural Science Foundation of China (21676188) and Key Projects in Natural Science Foundation of Tianjin (16JCZDJC37100) for support. JL acknowledges financial support by Marie Curie Fellowship from the European Union's Seventh Framework Programme (No. 291771) and the SNF-Nanotera RTD Project SYNERGY. MG. And SMZ thanks the King Abdulaziz City for Science and Technology (KACST) for financial support. Financial support from the Swiss National Science Foundation (SNSF), the NRP 70 "Energy Turnaround", CCEM-CH in the 9th call proposal 906: CONNECT PV, the European Union's Horizon 2020 research and innovation programme under the grant agreement No 687008 (GOTSolar) as well as from SNF-NanoTera and Swiss Federal Office of Energy (SYNERGY) is also gratefully acknowledged. The information and views set out in this article are those of the author(s) and do not necessarily reflect the official opinion of the European Union. Neither the European Union institutions and bodies nor any person acting on their behalf may be held responsible for the use which may be made of the information contained herein.

Received: ((will be filled in by the editorial staff))
Revised: ((will be filled in by the editorial staff))
Published online: ((will be filled in by the editorial staff))

[1] F. Zhang , S. R. Wang, X. G. Li , Y. Xiao , *Curr. Nanosci*. **2016**, *12*, 137.

[2] F. Zhang , X. Liu , C. Yi , D. Bi , J. Luo , S. Wang , X. Li , Y.Xiao , S. M. Zakeeruddin , M. Grätzel , *ChemSusChem*. **2016**, *9*, 2578.

[3] H. S. Jung , N.-G.Park , *Small*. **2015**, *11*, 10.

[4] W. S. Yang , J. H. Noh , N. J. Jeon , Y. C. Kim , S. Ryu , J. Seo , S. I. Seok, *Science*. **2015**, *348*, 1234.

[5] D. Q. Bi ,W. Tress, M. I. Dar , P. Gao , J .S .Luo, C. Renevier, K. Schenk,A. Abate, F. Giordano , J. C. Baena, J. Decoppet , S. M. Zakeeruddin , M. K. Nazeeruddin , M. Grätzel , A. Hagfeldt , *Sci. Adv.* **2016**, *2*, e1501170.

[6] T. A. Berhe, W. N. Su, C. H. Chen, C. J. Pan, J. H. Cheng, H. M. Chen, M. C. Tsai, L. Y. Chen, A. A. Dubaleb, B. J. Hwang, *Energy Environ. Sci*. **2016**, *9*, 323.

[7] NREL.Best Research-Cell Efficiencies, http://www.nrel.gov/ncpv/images/effi ciency_chart.jpg . (Dec **2016**)

[8] F. Zhang, C. Y. Yi, P. Wei, X. D. Bi, J. S. Luo,G. Jacopin, S. R. Wang, X. G. Li , Y. Xiao , S. M. Zakeeruddin, M. Grätzel , *Adv. Energy Mater*. **2016**, *6*,1600401.

[9] C. H. Chiang, C. G. Wu, *ChemSusChem*, **2016**, *9*,.2666.

[10] C.Y. Chang, W. K. Huang, Y. C. Chang, *Chem. Mater*, **2016**, *28*, 6305.

[11] M. Moriya, D. Hirotani, T. Ohta, Y. Ogomi, Q. Shen, T. S. Ripolles, K. Yoshino, T. Toyoda, T. Minemoto, S. Hayase, *ChemSusChem*, **2016**, *9*, 2634.

[12] M. D. McGehee, *Nat. Mater.*, **2014**, *13*, 845.

[13] T. A.Berhe, W.N.Su, C.H.Chen, C.J.Pan, J.-H.Cheng,H.M.Chen,M.C.Tsai, L.Y.Chen, A. A.Dubale, B.J.Hwang,*Energy Environ. Sci.* **2016**, *9*, 323.

[14] H. Tiep, Z. Ku, H. J. Fan, *Adv. Energy Mater.* **2016**, *6*, 1501420.

[15] D. Q. Bi, C. Y. Yi, J. S. Luo, J. D. Décoppet, F. Zhang, S. M. Zakeeruddin, X. Li, A. Hagfeldt , M. Grätzel, *Nature Energy*. **2016**, *1*, 16142.

[16] M. Salado, F. J. Ramos,V. M. Manzanares, P. Gao, M. K. Nazeeruddin, P. J. Dyson, S. Ahmad, *ChemSusChem*. **2016**, *9*, 2708.

[17] C. Liu, K. Wang, P. C. Du, C. Yi, T. Y. Meng ,X. Gong, *Adv.Energy Mater*. **2015**, *5*, 1402024.

[18] K. Wang, C. Liu, P. C. Du, J. Zheng,X. Gong, *Energy Environ. Sci.* **2015**, 8, 1245.

[19] C. H. Chiang, C. G. Wu, *Nat. Photonics*, **2016**, *10*, 196.

[20] J. J. Chang, Z. H. Lin, H. Zhu, F. H. Isikgor, Q. H. Xu,C. F. Zhang, Y. Hao, J. Y. Ouyang, *J. Mater. Chem. A*. **2016**, *4*, 16546.

[21] M. Saliba1, T. Matsui1, K. Domanski1, J. Y. Seo, A. Ummadisingu, S. M. Zakeeruddin, J-P. P. Correa-Baena, W. R. Tress, A, Abate, A. Hagfeldt, M. Grätzel, *Science*, **2016**, *354*, 206.

[22] M. Lenes, S.W. Shelton, A. B. Sieval, D. F. Kronholm, J. C. Hummelen, P. W. M. Blom, *Adv. Funct. Mater*. **2009**, *19*, 3005.

[23] Y. Matsuo, *Chem. Lett*. **2012**, *41*, 754.

[24] R. K. M.Bouwer, G. J. A. H. Wetzelaer, P. W. M. Blom, J.C.Hummelen, *J. Mater. Chem.* **2012**, *22*, 15412.

[25] Y. Kim, C. H. Cho, H. Kang, K. H. Kim, S. Park, T. E. Kang, K. Park, B. J. Kim, *Sol. Energ Mat. Sol. Cells*. **2015**, *141*, 87.

[26] W. Shi, X. Hou, T.Liu, X. Zhou, A. B. Sieval, J. C. Hummelen, T. J. S. Dennis, *Chem. Commun.*, **2017**, *53*, 975.

[27] M. Xiao, F. Huang, W. Huang, Y. Dkhissi, Y. Zhu, J. Etheridge, A. Gray-Weale, U. Bach, Y. B. Cheng, L. Spiccia, *Angew. Chem.* **2014**, *126*, 10056.

[28] J. Xu, A. Buin, A. H. Ip, W. Li, O. Voznyy, R. Comin, M. Yuan, S. Jeon, Z. Ning, J. J. McDowell, P. Kanjaaboos, J. P. Sun, X. Lan, L. N. Quan, D. H. Kim, I. G. Hill, P. Maksymovych, E. H. Sargent, *Nat. Commun.* **2015**, *6*, 7081.

[29] C.Li, J.Sleppy, N. Dhasmana, M.Soliman, L.Tetardd,J, Thomas, *J. Mater. Chem. A.* **2016**, *4*, 11648.

[30] T. Y. Zhang, N. J. Guo, G. Li, X. F. Qian, Y. X. Zhao, *Nano Energy*. **2016**, *26*, 50.

[31] Y. Tidhar, E. Edri, H. Weissman, D. Zohar, G. Hodes, D. Cahen, B. Rybtchinski, S. Kirmayer, *J. Am. Chem. Soc.* **2014**, *136*, 13249.

[32] M. Li, Z. K. Wang, Y. G. Yang, Y. Hu, S. L. Feng, J. M. Wang,X. Y. Gao, L. S. Liao, *Adv. Energy Mater.* **2016**, *6*, 1601156.

[33] Z. K. Wang, M. Li, Y. G. Yang, Y. Hu, H. Ma, X. Y. Gao, L. S. Liao, *Adv. Mater.* **2016**, *28*, 6695.

[34] Z. K. Wang, X. Gong, M. Li, Y. Hu, J. M. Wang, H. Ma, L. S. Liao, *ACS Nano*. **2016**, *10*, 5479.

[35] D. Q. Bi, P. Gao, R. Scopelliti, E. Oveisi, J. S. Luo, M. Grätzel, A. Hagfeldt, M. K. Nazeeruddin, *Adv. Mater.* **2016**, *28*, 2910.

[36] Y. Z. Wu, X. D.Yang, W. Chen,Y .F. Yue, M. L. Cai, F. X. Xie, E. B. Bi, A. Islam, L. Y. Han, *Nature Energy*, **2016**, *1*, 16148.

[37] Q. F. Dong, Y. J. Fang, Y. C. Shao, P. Mulligan, J. Qiu, L. Cao, J. S. Huang, *Science*, **2015**, *347*, 967.

[38] M. Li, Y. H. Chao, T. Kang, Z. K. Wang,Y. G. Yang, S. L. Feng, Y. Hu, X. Y. Gao, L. S. Liao, C. S. Hsu, *J. Mater. Chem. A.* **2016**, *4*, 15088.

[39] D. X. Yuan, A. Gorka, M. F. Xu, Z. K. Wang , L. S. Liao, *Phys. Chem. Chem. Phys.* **2015**, *17*, 19745.

[40] Y. Shao, Z. Xiao, C. Bi, Y. Yuan, J. S. Huang, *Nat. Commun*. **2014**, *5*, 5784.

[41] P. W. Liang, C. Y. Liao, C. C. Chueh, F. Zuo, S. T. Williams,X. K. Xin, J. Lin ,A. K. Y. Jen, *Adv. Mater.* **2014**, *26*, 3748.

[42] J. M. Frost, K. T. Butler, F. Brivio, C. H. Hendon,M. V. Schilfgaarde, A. Walsh, *Nano Lett.*, **2014**, *14*, 2584.

[43] R. Steim, S. A. Choulis, P. Schilinsky, U. Lemmer, C. J. Brabec, *Appl. Phys. Lett.* **2009**, *94*, 043304.

[44] Y. Yuan, J. S. Huang, *Acc.Chem. Res*. **2016**, *49*, 286.

[45] H. Back, G. Kim, J. Kim, J. Kong, T. K. Kim, H. Kang, H. Kim, J. Lee, S. Lee, K. Lee, *Energy Environ. Sci.* **2016**, *9*, 1258.

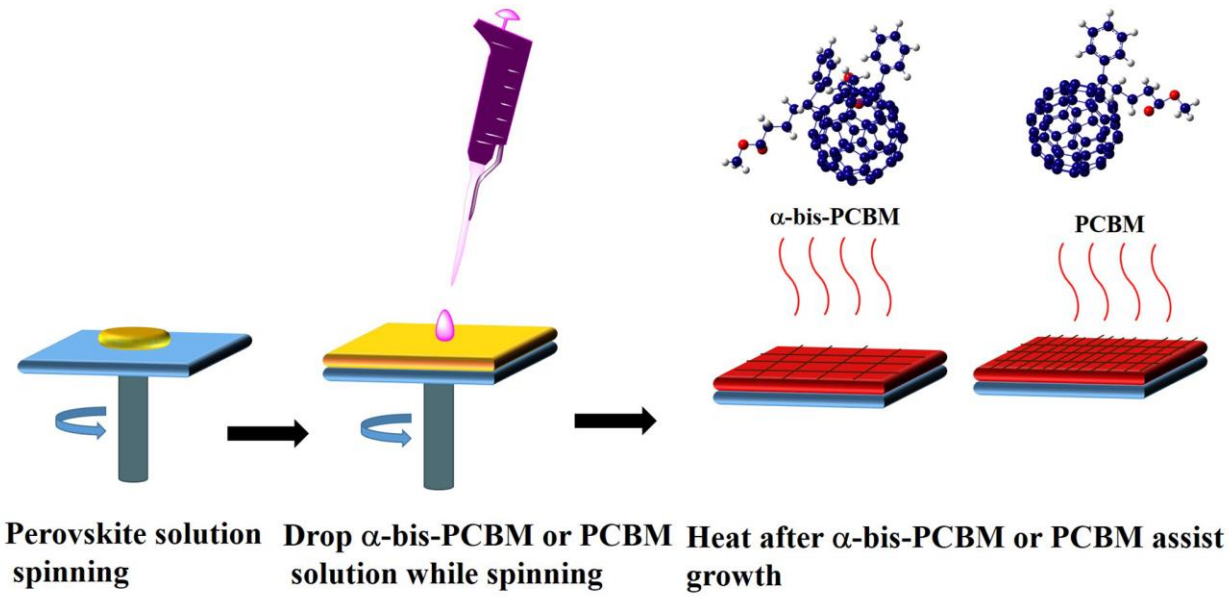

Figure 1 Schematic diagram of the α-bis-PCBM or PCBM-containing growth resulting in a perovskite- α–bis-PCBM or PCBM hybrid structure process flow for devices.

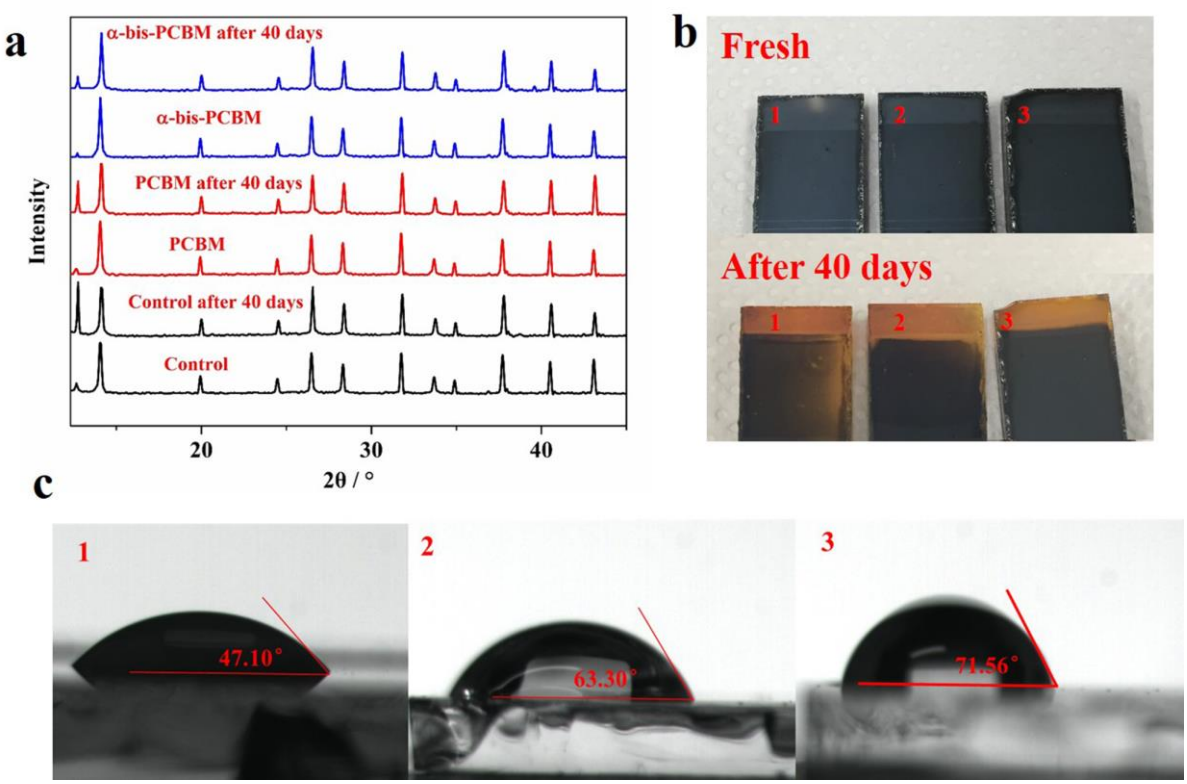

Figure 2 a) XRD patterns of corresponding films on meso-TiO_2/compact TiO_2/FTO substrate, which were exposed to ambient 40% relative humidity. b) The pictures of the corresponding films before and after aging to ambient 40% relative humidity. c) The contact angles between perovskite films and water: 1, Control; 2, PCBM; 3, α-bis-PCBM.

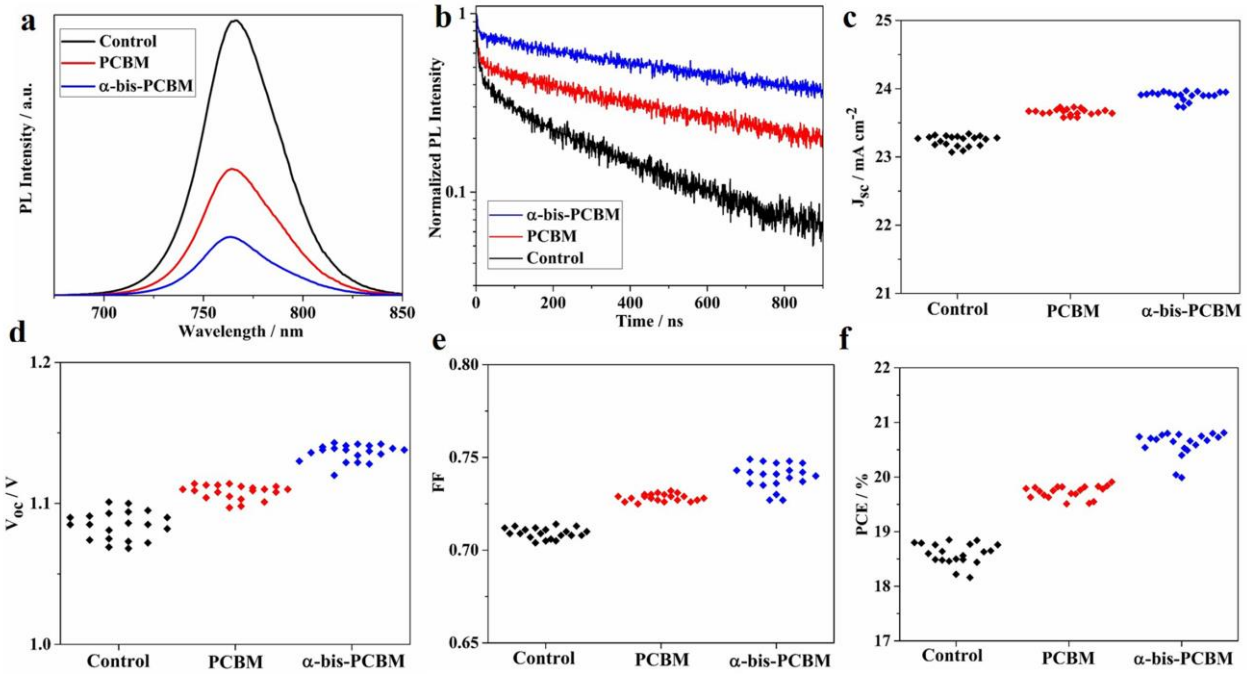

Figure 3 a) PL spectra, b) TRPL spectra of corresponding films on glass substrate. c), d), e), f) Photovoltaic metrics of devices based on corresponding perovskite layers.

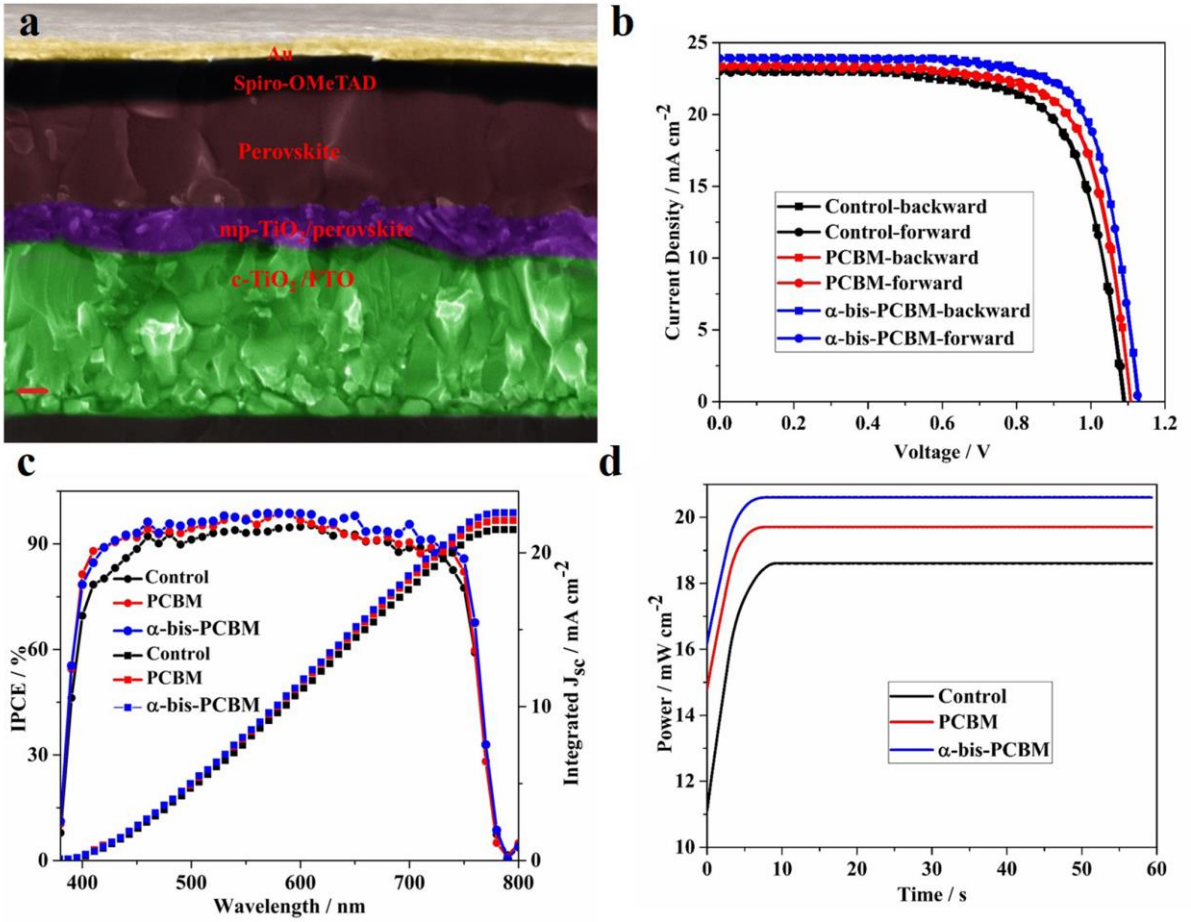

Figure 4 a) Cross-sectional SEM image of the device based on Bis-PCBM.The scale bar is 100 nm. b) Current-voltage hysteresis curves of perovskite solar cells comprising champion devices measured starting with backward scan and continuing with forward scan. c) IPCE spectra and integrated current curves of the corresponding devices. d) The stabilized power output of the corresponding devices.

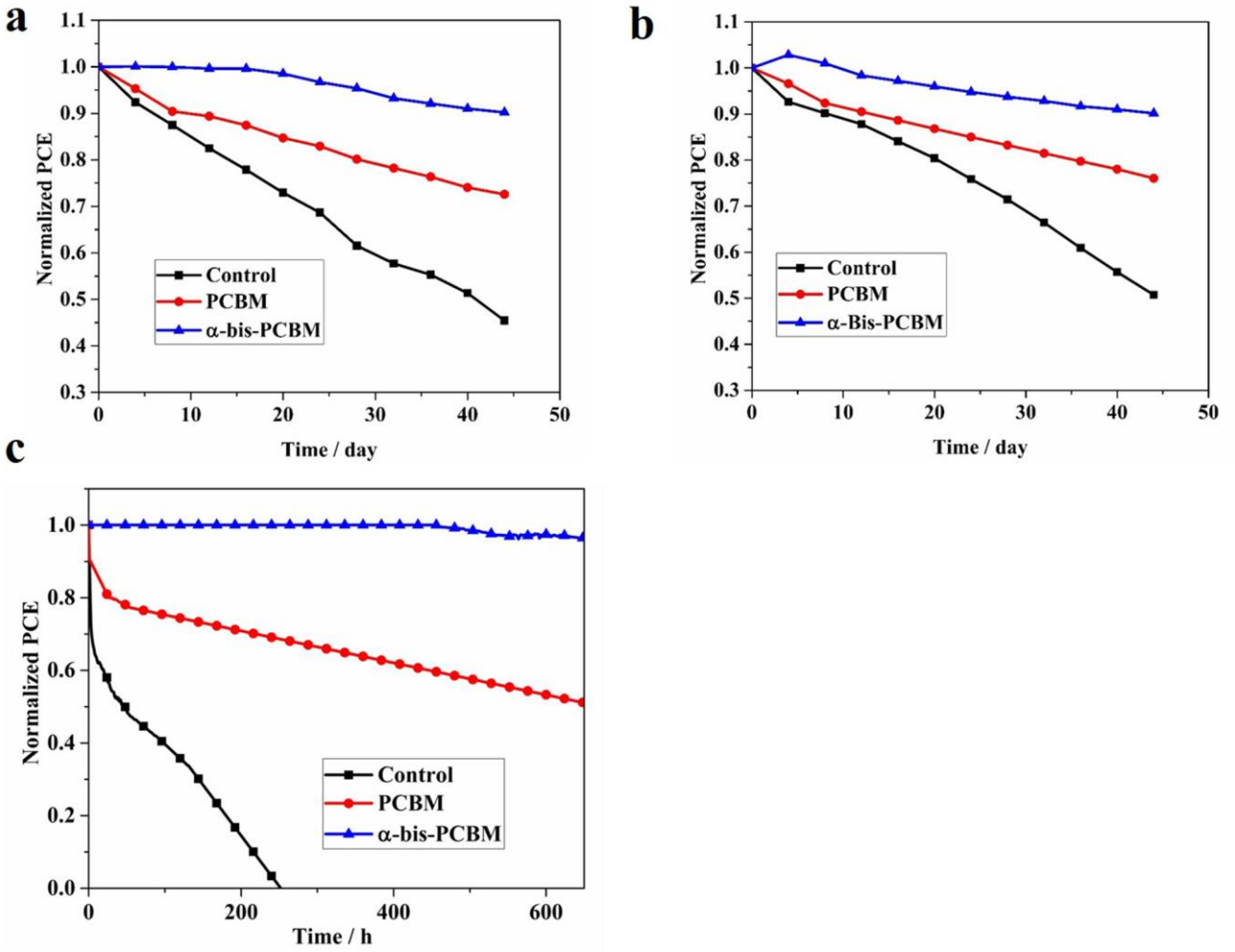

Figure 5 The stability of corresponding perovskite solar cells in ambient environment of 40% relatively humidity. a) Under dark without any encapsulation at room temperature. b) Under dark with encapsulation at 65℃. c) The stability of corresponding perovskite solar cells under continuous full sun illumination and maximum power point tracking in a nitrogen atmosphere at room temperature .